

Accepted Manuscript

Decarboxylation of Indomethacin Induced by Heat Treatment

Yohsuke Shimada, Haruki Komaki, Ayako Hirai, Satoru Goto, Yasuyuki Hashimoto, Hiromi Uchiro, Hiroshi Terada

PII: S0378-5173(18)30239-4
DOI: <https://doi.org/10.1016/j.ijpharm.2018.04.022>
Reference: IJP 17429

To appear in: *International Journal of Pharmaceutics*

Received Date: 26 January 2018
Revised Date: 23 March 2018
Accepted Date: 12 April 2018

Please cite this article as: Y. Shimada, H. Komaki, A. Hirai, S. Goto, Y. Hashimoto, H. Uchiro, H. Terada, Decarboxylation of Indomethacin Induced by Heat Treatment, *International Journal of Pharmaceutics* (2018), doi: <https://doi.org/10.1016/j.ijpharm.2018.04.022>

This is a PDF file of an unedited manuscript that has been accepted for publication. As a service to our customers we are providing this early version of the manuscript. The manuscript will undergo copyediting, typesetting, and review of the resulting proof before it is published in its final form. Please note that during the production process errors may be discovered which could affect the content, and all legal disclaimers that apply to the journal pertain.



Decarboxylation of Indomethacin Induced by Heat Treatment

Yohsuke Shimada^{1,2}, Haruki Komaki¹, Ayako Hirai¹, Satoru Goto^{1,2*}, Yasuyuki Hashimoto¹,

Hiromi Uchiro^{1,2} and Hiroshi Terada^{1,2}

¹*Faculty of Pharmaceutical Sciences, Tokyo University of Science, 2641 Yamazaki, Noda, Chiba 278-8510, Japan*

²*Center for Drug Delivery Research, Faculty of Pharmaceutical Sciences, Tokyo University of Science, 2641 Yamazaki, Noda, Chiba 278-8510, Japan*

*To whom correspondence should be addressed: s.510@rs.tus.ac.jp

Abbreviations used: COSY, correlated spectroscopy; DEPT, distortionless enhancement by polarization transfer; DSC, differential scanning calorimetry; DTA, differential thermal analysis; EI, electron ionization; HMQC, heteronuclear multiple quantum coherence; INM, indomethacin; MS, mass spectrometry; SEM, scanning electron microscopy; TG, thermogravimetry; XRPD, X-ray powder diffraction.

ABSTRACT

As crystalline indomethacin is heated and subsequently cooled, it transforms into glassy indomethacin. While the original crystals are off-white in color, the glass becomes blackish-brown via a yellow intermediate stage. TLC of the components of the glass revealed three bands. The yellow component, which is generated either under hypoxic conditions or in the dark, was elucidated by NMR spectroscopy to be a decarboxylated fragment produced by thermal degradation. The colorless component is proposed to be formed by the opening of the indole ring of indomethacin; the structure of this degradation product was identified by EI-MS to be the same as the oxidative-cleavage product formed upon UV-irradiation, as previously reported. Another band was a blackish-brown pigment whose mobility placed it close to the TLC baseline. This oxidative-cleavage product and the blackish-brown pigment are not generated under hypoxic conditions. However, the extent of indomethacin decarboxylation under hypoxic conditions was found to be dependent on the heating temperature and time. Consequently, we prepared amorphous indomethacin through control of the heating temperature and time; heating at 160 °C for 30 min or less under hypoxic conditions is optimum for obtaining pure amorphous indomethacin.

Keywords: indomethacin, amorphous, decarboxylation, NMR, EI-MS

1. INTRODUCTION

Compounds belonging to the arylalkanoic acid family derived from 2-arylacetic acids, such as indomethacin, sulindac, diclofenac, and tolmetin, and those derived from 2-arylpropionic acids, such as naproxen, ibuprofen, fenoprofen, ketoprofen, flurbiprofen, and loxoprofen, are anti-inflammatory, antipyretic, and analgesic agents. These non-steroidal anti-inflammatory drugs (NSAIDs) are clinically effective in the therapy of inflammation, chronic rheumatoid arthritis, peri-arthritis, osteoarthritis, spondylosis deformans, and acute gout, by inhibiting cyclooxygenase (COX), an enzyme belonging to the prostaglandin synthetic cascade. Indomethacin (INM) is a commonly used effective NSAID. Its abilities and photoproducts to scavenge hydroxyl radicals and inhibit xanthine oxidase have also been reported (Lien et al., 2013). Other NSAIDs, such as ketoprofen, have also been reported to have radical-scavenging abilities, these NSAIDs also present photosensitivity as a side effect of their photolysis (Takara et al., 2017). However, INM is sparingly soluble in aqueous media. Therefore, there have been numerous attempts to improve its water solubility. One well-documented method is to make INM amorphous, which could be accomplished by the heating quenching method or hot melt extrusion method (ElShaer et al., 2011; Forster et al., 2001; Inada et al., 2013; Jung et al., 2010; Kawakami et al., 2004; Shimada et al., 2013a, 2013b; Shimada et al., 2018).

Amorphous INM is readily obtained by the heat treatment of crystalline INM at temperatures above its melting point, followed by cooling of the fused INM. Heat-treated INM does not crystallize following cooling, and exhibits a transition to the glass state at about 42 °C (Shimada et al., 2013a). In addition, heat treatment of crystalline INM results in a change in color; off-white crystalline INM turns yellow upon melting and then blackish brown. Despite being known for some time, the mechanism associated with these color changes is unclear (Shimada et al., 2013a).

This study investigated the mechanism of the heat-induced color change of INM by

means of scanning electron microscopy (SEM), thermogravimetry/differential-thermal analysis (TG/DTA), differential scanning calorimetry (DSC), X-ray powder diffraction (XRPD), thin-layer chromatography (TLC), electron-ionization mass spectrometry (EI-MS), and nuclear magnetic resonance (NMR) spectroscopy.

2. MATERIALS AND METHODS

2.1 Materials

Crystalline INM was purchased from Wako Pure Chemical Industries, Ltd. (Osaka, Japan). Glass TLC plates, coated with silica gel and F₂₅₄ fluorescent indicator, were obtained from Merck (Darmstadt, Germany). Other chemicals and solvents were of reagent grade and commercially available.

2.2 Preparation of the glass form of INM

In a typical procedure, 20 mg of crystalline INM was heated at 200 °C for 1, 5, 15, 30, or 60 min in a sample tube immersed in an oil bath to form fused INM, after which it was cooled to room temperature to obtain glassy INM. Heating and cooling were performed either under aerobic or hypoxic conditions, which were achieved by purging the air inside the sample tube with argon.

2.3 SEM

The scanning electron micrographs of crystalline INM and glass form of INM (which was heated at 200 °C for 1 or 60 min) were taken using a miniscope (TM-1000; Hitachi High-Technologies Co., Tokyo, Japan). Samples were fixed on a sample holder with conductive double-sided adhesive tape. The operating conditions were: accelerating voltage 15 kV and scanning time 40 s. The glassy samples were crushed with an agate mortar and pestle into powder before measurements.

2.4 DSC and XRPD

Thermal analyses were performed using a DSC8230 instrument (Rigaku Co., Tokyo, Japan)

with 10 mg of INM placed in an aluminum pan. After the pan was sealed, the temperature was scanned between -40 and 170 °C at 10 °C/min, using the onset temperature as the melting temperature. XRPD analyses were performed in parallel with the DSC measurements on a RINT2000 X-ray diffractometer (Rigaku Co.) with Cu $K\alpha_1$ radiation, operating at 40 kV and 40 mA in the 10 – 40° 2θ range, with scanning at 15 °/min.

2.5 TLC

The crystalline and glass forms of INM were dissolved in 2 mL of acetonitrile. Samples were developed on TLC plates with ethyl acetate as the eluent, and were visualized under ultraviolet light (254 nm). In addition, the separated products were extracted by preparative TLC method using a sufficient amount of chloroform as eluent.

2.6 NMR spectroscopy and EI-MS

Crystalline INM and the corresponding fused samples were dissolved in 1 mL of chloroform- d_1 and filtered through cotton mesh to provide a solution for ^1H -NMR and ^{13}C -NMR spectroscopy. The structures of INM and decarboxylated INM were assigned by ^1H - ^1H -COSY, and HMQC techniques, which are more accurate NMR methods. Spectra were acquired using an LA-400 NMR spectrometer (JEOL Ltd, Tokyo, Japan) using tetramethylsilane as an internal reference. EI-MS studies were performed on a Varian 910-MS TQ-FT-ICR mass spectrometer (JASCO International Co. Ltd., Tokyo, Japan).

2.7 Preparation of intact glassy INM

In a typical experiment, 20 mg of crystalline INM in a sample tube was heated in an oil bath at predetermined temperatures and heating times under hypoxic conditions, after which it was cooled to room temperature to obtain glassy INM.

2.8 Solubility of crystalline or amorphous INM

The crystalline and glassy forms of INM were added to a sodium citrate-hydrochloric acid buffer (pH 1.2) and shaken in a water bath at 310 K for 120 min. The supernatant was then filtered using a membrane filter (Minisart RC 4, 0.20 μm ; Sartorius, Göttingen, Germany). The concentration of

INM in the supernatant was determined using HPLC (Shimadzu Co., Kyoto, Japan), with a mobile phase of acetonitrile:tetrahydrofuran:acetic acid:ultrapure water (50:5:0.2:44.8 v/v/v/v) and a flow rate of 1 mL·min⁻¹ using a reversed phase column (Capcell Pak C18; Shiseido; 5 µm, 4.6 mm Φ×250 mm) at 313 K. The amount of INM was determined by monitoring the absorbance at 320 nm. Curve fitting was carried out by using Microsoft Office excel solver module (Microsoft Co., Redmond, USA).

3. RESULTS

3.1 Changes in State and Color of Indomethacin upon Heat Treatment

Heating crystalline INM at temperatures above its melting temperature (160 °C; Shimada et al., 2013a, 2013b) resulted in a color change, from off-white crystals to pale yellow and then blackish-brown, depending on the heating temperature and time, with the INM melt becoming a paste. Figure 1a shows photographic images of INM after heating at 200 °C under aerobic conditions for various times. Upon heating, a transparent yellow paste was obtained

Figure 1

in a few minutes, after which it turned brown and then blackish-brown. DSC of INM over the -40 °C to 170 °C range at 10 °C/min revealed an endothermic peak at 160 °C that corresponds to the melting of INM. However, no exothermic peak was observed upon cooling of the fused INM to -40 °C; instead a transition signal due to the formation of the glassy state was observed at 42 °C, as reported recently by us (Shimada et al., 2013a, 2013b). Although signals specific to the crystalline form were observed in the XRPD pattern of crystalline INM, fused INM exhibited halo-patterns characteristic of the amorphous state (see Supplemental Data). From the DSC and XRPD results, cooling of the fused INM crystals results in the formation of the amorphous state. However, as shown in Figure 1b, there was no qualitative morphology change in the SEM image of INM after it became amorphous (following 1 and 60 min of heating).

Although the particle size of the crystal INM (γ type) is small, it did not have a characteristic form in its crystal habit.

Table 1

3.2 Structural Changes of Indomethacin upon Heating

To elucidate which chemical species are generated by heating INM, the crystalline and heat-treated INM samples were subjected to TLC with ethyl acetate as the eluent. As shown in Fig. 2, heat-treated INM exhibits three distinct spots, with R_f values of 0.667, 0.478, and 0.289. Of these, the spot at R_f 0.289 is apparently due to INM because the same R_f was observed for the spot corresponding to crystalline INM. The major ($R_f = 0.667$) and minor ($R_f = 0.478$) spots should correspond to the products generated by the heat treatment of INM; and these products are referred to as Product-1 and -2, respectively. In addition, a thin smear was observed from the baseline to the solvent front of the TLC plate for the amorphous INM sample, and an amount of blackish-brown material remained at the baseline. We refer to these blackish-brown species, as a whole, as “blackish-brown pigments.” Product-1 was yellow in color, as observed by the spot corresponding to the INM crystals, whereas Product-2 was colorless. Hence, the blackish-brown color of heat-treated INM is due to the blackish-brown pigments rather than Product-1 or -2.

Figure 2

We retrieved Product-1 and -2 by preparative TLC using chloroform as the eluent. The ^{13}C -NMR spectrum of Product-1 in chloroform- d_1 reveals that the signals corresponding to C-11 (δ 30.01) and C-12 (δ 176.77) of the dissolved crystalline INM were absent, with a new signal appearing at δ 8.77 (Table 1). The “lost” C-11 and C-12 signals correspond to the C-11-methylene and C-12-carboxyl groups in crystalline INM, with the “new” signal corresponding to a methyl group. MS reveals that Product-1 has a MW 313.1. These spectra, as well as those acquired by ^1H -NMR, ^1H - ^1H -COSY, and HMQC spectroscopy, reveal that the

major component (Product-1) in the heat-treated INM is the decarboxylated INM, as was observed when INM was photochemically degraded (Weedon and Wong, 1991). INM and Product-1 are yellow due to conjugation between their indole rings and amide groups.

The EI-MS spectrum suggests that Product-2 has a MW of 288.0. We attempted to identify the chemical structure of Product-2; however, the amount of Product-2 recovered was too low for NMR spectra to be acquired. As Product-2 is colorless, it is possible that the original indole ring in INM may have been oxidatively destroyed. Wu et al. determined the chemical structure of their photoproduct to be a 1,2-dioxane derivative with a 6-membered ring bridging the 2nd and 3rd positions of the indole ring, which was produced by UV irradiation and oxygen via an acyl radical. EI-MS and NMR spectroscopy revealed that the compound with a MW of 288.0 was a fragment ion produced through the cleavage of the indole ring in the 1,2-dioxane derivative by electron collision during EI-MS (Wu et al., 1997); therefore, we consider Product-2 to correspond to this fragment. In addition, it was very difficult to isolate sufficient quantities of the blackish-brown pigments for characterization by NMR spectroscopy and MS because their extractions with various solvents, such as methanol, ethanol, ethyl acetate, acetone, acetonitrile, or phosphate buffer (pH 7.4), proved to be very difficult. Hence, we were unable to establish the chemical structural changes that take place in INM upon heating to form the blackish-brown pigments. However, the blackish-brown pigments are likely to be polyphenols and/or polymers with quinone structures that are produced by the oxidation of INM to produce the quinone derivative of *p*-anisidine (*p*-aminoanisole), as suggested by the photochemical degradation of INM (Weedon and Wong, 1991).

3.3 Heat Treatment of Indomethacin under Hypoxic Conditions

As oxygen was thought to trigger the polymerization of INM, we subsequently heat treated INM under hypoxic conditions by replacing air with argon gas. INM heat-treated at 200 °C for 60 min under hypoxic conditions was yellow in color, in contrast to the

blackish-brown color following heat treatment under aerobic conditions. Hence, the blackish-brown color of the product formed under aerobic conditions is proposed to be due to the oxidative polymerization of INM. In addition, the TLC plate of INM following heating under hypoxic conditions exhibited two spots, the R_f values of which were identical to those of intact INM and Product-1 obtained by heat treatment under aerobic conditions. In addition, the colors of the Product-1 bands following the heat treatment of INM under hypoxic and aerobic conditions were the same. We confirmed by NMR spectroscopy that Product-1 obtained by heating under hypoxic and aerobic conditions were identical. Hence, Product-2, as well as blackish-brown pigments formed by heating under aerobic conditions, is a product from the oxidation of INM.

Product-1 is proposed to be decarboxylated INM based on ^{13}C - and ^1H -NMR spectroscopy and MS. Scheme 1 displays a possible mechanism for the heat-induced decarboxylation of INM under both hypoxic and aerobic conditions. The 10- π -electron ring system of INM is interrupted by protonation from the carboxylic acid at C-12, which attacks C-2 carbon, adjacent to the nitrogen atom. INM then decarboxylates leading immediately to Product-1 via an unstable intermediate structure. It is noteworthy that only Product-1 was produced (without the formation of any Product-2) during the photochemical decarboxylation of INM (Weedon and Wong, 1991). This indicates that the mechanism depicted in Scheme 1 and that for the formation of Product-2 are complementary; hence Product-1 is rapidly produced without the need for additional high energy, such as that produced during EI-MS.

Scheme 1

3.4 Temperature Dependence of the Degradation of Indomethacin

We next examined the dependence of Product-1 formation on heating temperature and heating time under hypoxic conditions. With increasing temperature and heating time, the “new”

signal at 2.19 ppm in the $^1\text{H-NMR}$ spectrum of the decarboxylated product, due to the three methyl protons at C-(11), increased synchronously with the decrease observed for the peak at 3.69 ppm corresponding to the two methylene protons at C-11 of the intact INM. The signals at 2.19 ppm and 3.69 ppm are referred to as “S1” and “S2”, respectively. As the areas of S1 (IV_{S1}) and S2 (IV_{S2}), obtained by peak integration, represent the relative amounts of Product-1 and the original intact INM, respectively, we determined the amount of Product-1 relative to the original amount of INM using the equation given below.

$$\text{Amount of Product-1 generated (\%)} = IV_{S1}/3/(IV_{S1}/3 + IV_{S2}/2) \times 100$$

Figure 3 shows the percentage of Product-1, generated by heating for 60 min under hypoxic conditions, as a function of temperature. The decarboxylation of INM begins at its melting temperature (T_m , 160 °C), and progressively increases with increasing temperature, reaching about 30% at 200 °C. When INM was heated at 200 °C for various times under hypoxic conditions, the percentage of Product-1 increased linearly with increasing heating time, as shown in Fig. 4. As the generation of Product-1 is both dependent on heating temperature and time, it is possible to determine conditions that avoid its production. After examination of the amounts of Product-1 generated at various heating temperatures and times under hypoxic conditions, we found INM begins to degrade to form Product-1 at the T_m of INM (160 °C) after heating for 40 min or longer; above T_m the degradation of INM proceeds more rapidly with increasing heating time, and Product-1 is instantaneously generated at 200 °C. Figure 5 summarizes the relationship between heating temperature and heating time for the preparation of amorphous INM under hypoxic conditions. Clearly, amorphous INM, devoid of any Product-1, Product-2, or blackish-brown-pigment impurities, can be obtained under hypoxic conditions through control of the heating temperature and time, as shown by the data in Fig. 5. Product-1 was generated by heating INM at 160 °C for more than 40 min, at 170 °C for more

than 10 min, and at 180 °C for more than 5 min; heating at 160 °C for 30 min or less under hypoxic conditions is optimum for obtaining pure amorphous INM. When INM is heated under aerobic conditions, Product-1, Product-2, and the blackish-brown component are not produced when heated at 160 °C for less than 2 min, and at 170 °C for less than 1 min.

Figure 3, Figure 4, Figure 5

Figure 6 shows the solubility data of γ type and amorphous INM at 25 °C and pH 1.2. Amorphous INM was prepared by heating at 170 °C for about 5 min in the shaded range shown in Fig. 5 and cooling to room temperature. In this experiment, since INM (pK_a 4.3) exists in the molecular form in solution, the saturation value after 120 min is its solubility. From the literature, the INM solubility is improved several times as it becomes amorphous, which was seen in this experiment as well.

Figure 6

4. DISCUSSION

We heated crystalline INM above its melting point of 160 °C under aerobic conditions for specific times, which resulted in the formation of two species, namely Product-1 and -2, which were yellow and colorless, respectively, as well as blackish-brown pigments. Product-1 was determined to be decarboxylated INM, while Product-2 corresponded to the fragment ion obtained by cleavage of the indole ring in a 1,2-dioxane derivative by EI-MS (Wu et al., 1997). However, heating INM under hypoxic conditions generated only Product-1, with no Product-2 or blackish-brown pigments formed, indicating that the blackish-brown color of heat-treated INM is mainly due to polyquinones produced by the oxidation of the *p*-aminoanisole moiety of INM, as observed during the photochemical degradation of INM (Weedon and Wong, 1991; Wu et al., 1997). Product-1 and Product-2 are generated through different pathways; Product-1 is produced only by heating, while Product-2 is produced by heat and oxygen, which behaves as a

catalyst for the formation of the blackish-brown pigment.

The rate of formation of Product-1 through the decarboxylation of INM above its T_m (160 °C) depends on the heating temperature and the heating time. The degradation of INM at a fixed heating temperature increased with time in a linear manner. In addition, Figure 5 reveals the times over which uncontaminated amorphous INM was formed at each temperature. For example, INM was stable at 160 °C for up to 30 min, while at 200 °C it took only 1 min for degradation to occur. It is noteworthy that the decarboxylation of INM is temperature dependent, and that the reaction essentially does not occur after cooling to room temperature in the absence of UV irradiation. Therefore, we were able to prepare uncontaminated stable amorphous INM by controlling the heating temperature and time.

The reason why the melted INM is yellow in color is unknown; however the thermal decomposition results provide clues. Since amorphous INM and Product-1 are yellow in color but crystalline INM and Product-2 are not, the yellow color might be due to the degree of indole-ring conjugation and the resonance structures formed, which depend on flexible conformation not present in the crystalline form. Regardless of decarboxylation, the color depends on whether the indole ring and the benzene ring form a crystal structure. The color is yellow for the flexible amorphous form, but off-white for the rigid crystal form. In particular, we believe that the dihedral angle between indole ring and benzene ring affects yellow.

The water solubility of INM is greatly improved by changing its state from crystalline to amorphous; however amorphous INM is decomposed by light as well as heat. We examined the degradation of INM by changing the heating temperature and time. This revealed that amorphous INM is readily obtained without decomposition under appropriate conditions. In addition, it has been suggested that the heat-decomposition products are reactive toward radicals. Since the presence of free radicals may induce the decomposition of amorphous INM, it is also important to consider protecting INM against free radicals.

5. REFERENCES

- ElShaer, A., Khan, S., Perumal, D., Hanson, P., Mohammed, A.R., 2011. Use of amino acids as counterions improves the solubility of the BCS II model drug, indomethacin. *Curr. Drug. Deliv.* 8, 363–72.
- Forster, A., Hempenstall, J., Tucker, I., Rades, T., 2001. Selection of excipients for melt extrusion with two poorly water-soluble drugs by solubility parameter calculation and thermal analysis. *Int. J. Pharm.* 226, 147–161.
- Hawkey, C.J., 2000. Non-steroidal anti-inflammatory drug gastropathy. *Gastroenterology* 119, 521–535.
- Inada, A., Oshima, T., Takahashi, H., Baba, Y., 2013. Enhancement of water solubility of indomethacin by complexation with protein hydrolysate. *Int. J. Pharm.* 453, 587–593.
- Jung, M.S., Kim, J.S., Kim, M.S., Alhalaweh, A., Cho, W., Hwang, S.J., Velaga, S.P., 2010. Bioavailability of indomethacin-saccharin cocrystals. *J. Pharm. Pharmacol.* 62, 1560–1568.
- Kawakami, K., Miyoshi, K., Ida, Y., 2004. Solubilization behavior of poorly soluble drugs with combined use of Gelucire 44/14 and cosolvent. *J. Pharm. Sci.* 93, 1471–1479.
- Lien, G.S., Chen, C.S., Chen, W.Y., Huang, S.H., Cheng, K.T., Lin, C.M., Chao, S.H., 2013. Photoproducts of indomethacin exhibit decreased hydroxyl radical scavenging and xanthine oxidase inhibition activities. *J. Food Drug Anal.* 21, 332–336.
- Shimada, Y., Goto, S., Uchiro, H., Hirabayashi, H., Yamaguchi, K., Hirota, K., Terada, H., 2013a. Features of heat-induced amorphous complex between indomethacin and lidocaine. *Colloids Surf. B Biointerfaces* 102, 590–596.
- Shimada, Y., Goto, S., Uchiro, H., Hirota, K., Terada, H., 2013b. Characteristics of amorphous complex formed between indomethacin and lidocaine hydrochloride. *Colloids Surf. B Biointerfaces* 105, 98–105.
- Shimada, Y., Tateuchi, R., Chatani, H., Goto, S., 2018. Mechanisms underlying changes in indomethacin solubility with local anesthetics and related basic additives. *J. Mol. Struct.* 1155,

165–170.

Takara, A., Kobayashi, K., Watanabe, S., Okuyama, K., Shimada, Y., Goto, S., 2017. Dibucaine inhibits ketoprofen photodegradation via a mechanism different from that of antioxidants. *J. Photochem. Photobiol. A Chem.* 333, 208–212.

Weedon, A.C., Wong, D.F., 1991. The photochemistry of indomethacin. *J. Photochem. Photobiol. A Chem.* 61, 27–33.

Wehling, M., 2014. Non-steroidal anti-inflammatory drug use in chronic pain conditions with special emphasis on the elderly and patients with relevant comorbidities: management and mitigation of risks and adverse effects. *Eur. J. Clin. Pharmacol.* 70, 1159–1172.

Wu, A.B., Cheng, H.W., Hu, C.M., Chen, F.A., Chou, T.C., Chen, C.Y., 1997. Photolysis of indomethacin in methanol. *Tetrahedron Lett.* 38, 621–622.

Figure captions

Figure 1. (a) Photographic images of crystalline INM (0 min) in a sample tube, and the color changes observed for fused INM heated at 200 °C for 1, 5, 15, 30, and 60 min under aerobic conditions. (b) Left to right: SEM images of crystalline INM (0 min, x1000 and x2000), of fused INM heated at 200 °C for 1 min (x500) and 60 min (x1000) under aerobic conditions, during the color change shown in (a).

Figure 2. Thin-layer chromatograms. Left lane: INM (R_f 0.289). Right lane: three distinct spots for fused INM; Product-1 (R_f 0.667), Product-2 (R_f 0.478), and the blackish-brown pigment (baseline).

Figure 3. The dependence of the formation of Product-1 on heating temperature at 60 min under hypoxic conditions. The degradation rate is calculated by $(IV_{S1/3})/(IV_{S1/3} + IV_{S2/2}) \times 100$ and IV values are obtained from $^1\text{H-NMR}$ data.

Figure 4. The dependence of the formation of Product-1 on heating time. INM was heated at 200 °C for various times under hypoxic conditions. The degradation rate was calculated using $(IV_{S1/3})/(IV_{S1/3} + IV_{S2/2}) \times 100$, and IV values are obtained from $^1\text{H-NMR}$ data.

Figure 5. The relationship between heating temperature and heating time for the formation of amorphous INM devoid of Product-1, Product-2, and the blackish-brown pigments, under hypoxic conditions.

Figure 6. Solubility of the γ -form (diamonds and gray line) and amorphous form (circles and black line) of INM in citric acid buffer (pH 1.2). Error bars are standard deviations for $n = 3$, except for those at 5, 15, and 90 min in γ INM ($n = 2$). The lines were constructed by curve

fitting using Excel solver module.

Scheme caption

Scheme 1. Mechanism for the heat-induced decarboxylation of INM.

ACCEPTED MANUSCRIPT

Table 1. Molecular structures of INM and decarboxylated INM, and their $^1\text{H-NMR}$ and $^{13}\text{C-NMR}$ chemical shifts in chloroform- d_1 . The integrated values (*IVs*) were determined against the $^1\text{H-NMR}$ peaks of H-7, which correspond to one proton.

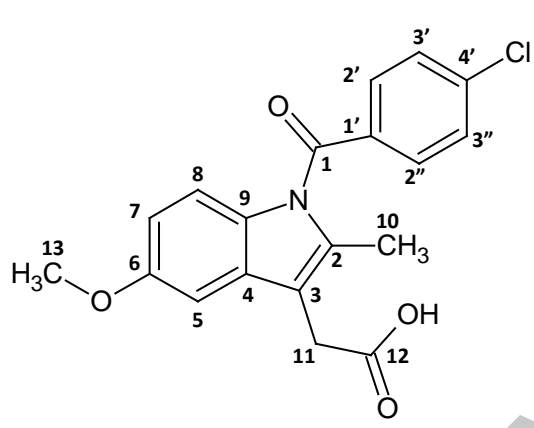
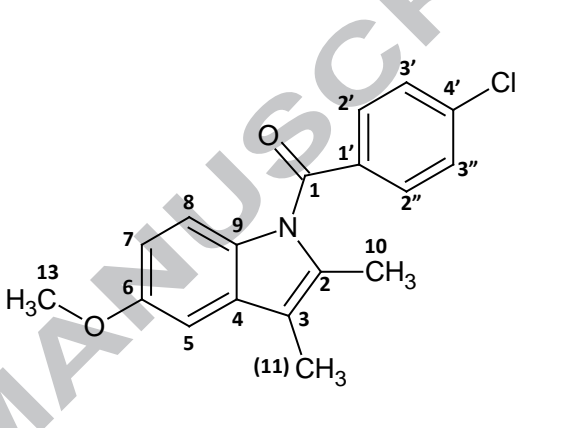
INM				Decarboxylated INM			
							
No.	$^1\text{H-NMR}$	<i>IV</i>	$^{13}\text{C-NMR}$	No.	$^1\text{H-NMR}$	<i>IV</i>	$^{13}\text{C-NMR}$
1			168.310	1			168.253
2			136.266	2			134.390
3			111.823	3			115.435
4			130.466	4			130.877
5	6.944(d)	1.00	101.259	5	6.892(d)	1.90	101.292
6			156.068	6			155.962
7	6.667(dd)	1.00	111.700	7	6.661(dd)	1.00	111.157
8	6.849(d)	1.01	115.007	8	6.892(d)	1.90	114.933
9			130.787	9			131.963
10	2.380(s)	2.91	13.295	10	2.311(s)	2.79	13.311
11	3.685(s)	2.02	30.013	11	-	-	-
12			176.768	12			-
13	3.820(s)	3.06	55.731	13	3.848(s)	3.13	55.731
1'			133.798	1'			133.789
2'(2'')	7.656(td)	2.06	131.198	2'(2'')	7.641(t)	2.22	131.042
3'(3'')	7.462(td)	2.04	129.149	3'(3'')	7.461(t)	2.08	129.034
4'			139.351	4'			138.874
				(11)	2.192(s)	3.22	8.770

Figure 1

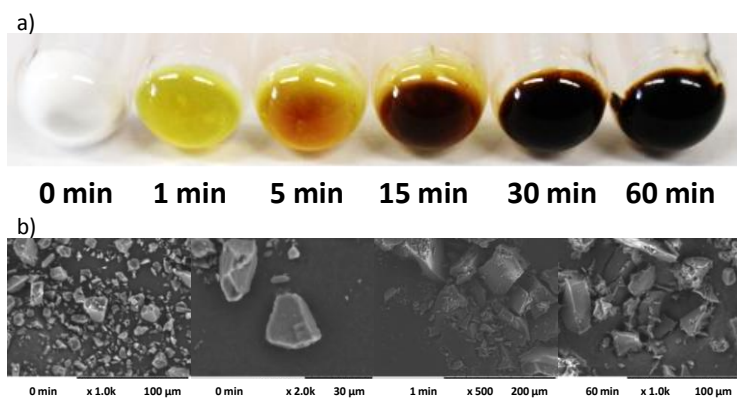


Figure 2

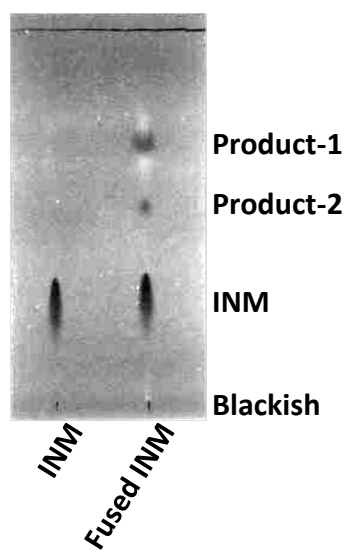


Figure 3

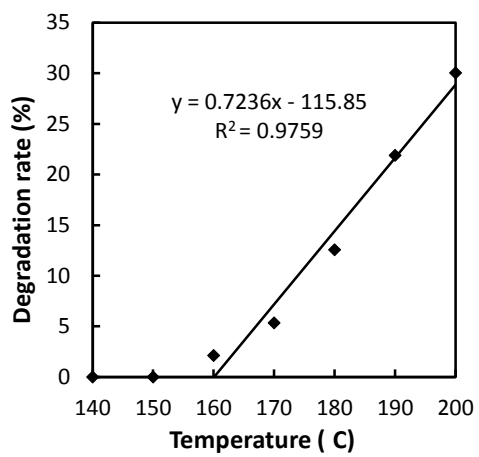


Figure 4

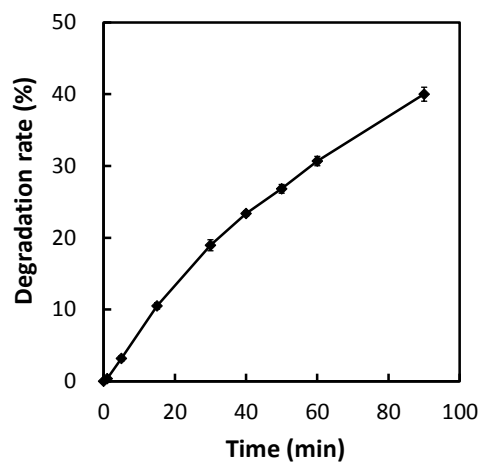


Figure 5

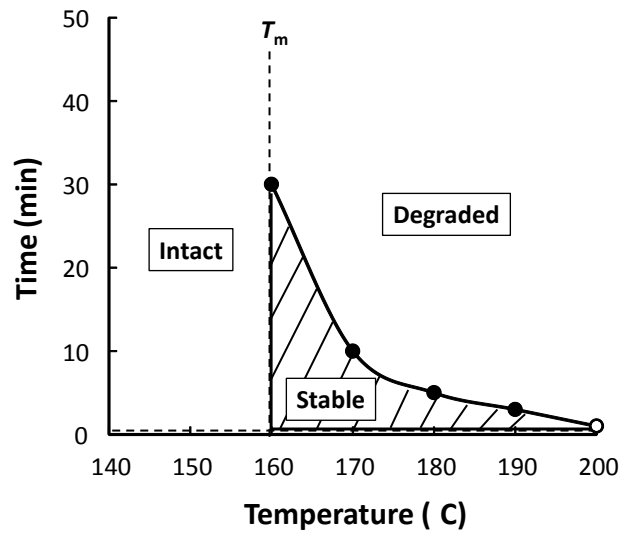
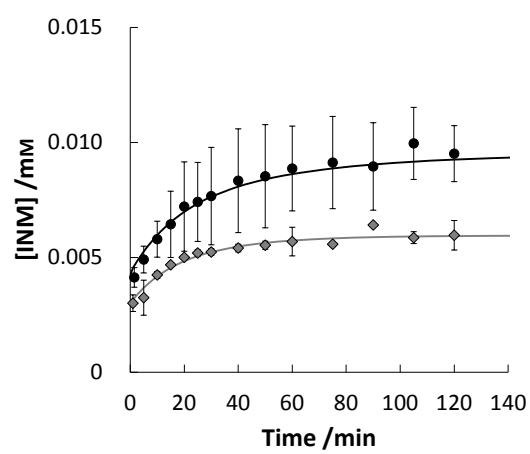


Figure 6



ACCEPTED

ACCEPTED MANUSCRIPT

Scheme 1

